Research paper

A case study on tunnel blasting design evaluation considering blast damage zone

Seong-Seung Kang* and Hyongdoo Jang** †

*Department of Energy & Resources Engineering, Chosun University, Gwangju 61452, REPUBLIC OF KOREA

**Western Australian School of Mines: Minerals, Energy and Chemical Engineering, Curtin University,
  WA, 6430, AUSTRALIA
  Phone: +61 8 9088 6177
†Corresponding author: Hyongdoo.jang@curtin.edu.au

Abstract

　Hard rock tunnel blasting becomes more efficient with the state-of-the-art technology advancements of the computer-aided drilling machine which minimises the drilling error. However, overbreak is still considered as the primary challenge of any tunnelling project using drilling and blasting methods. This study evaluates a standard tunnel blasting design for 1 m advance used in a tunnel construction site in Japan. Blast damage zone (BDZ) of a single buffer hole blast design of the tunnel is estimated using Ash's modified energy and pressure-based approaches which calculated as 0.81, and 0.95 m respectively. In succession, five numerical models with different tunnel perimeter spacing-to-burden (*S/B*) ratio were simulated using ANSYS AUTODYN to evaluate *S/B* ratio effects to damages beyond the tunnel contour. The average practical BDZ of the AUTODYN analyses was estimated at 0.83 m which is reasonably corresponding with the Ash's BDZ approaches. The results show that more damages caused when *S/B* ratio increases. When the perimeter space is fixed to 0.83 m, the most appropriate *S/B* ratio is 1.0 for the tunnel construction site. The presented process of the BDZ evaluation can be applied in tunnel blasting designs in practice to minimise possible overbreak.

Keywords: blast damage zone, buffer concept, tunnel, overbreak, AUTODYN

1. Introduction

　Overbreak is one of the principal challenges to underground civil and mining projects when drilling and blasting methods are applied to excavate rock mass. Such a phenomenon has long been recognised as an inevitable consequence of blasting and its management directly influences not only the safety but also the productivity of the project[1]. In practice, it is difficult to keep the overbreak under a management limit if the quality of rock mass is poor. The causing mechanism of overbreak is highly complex where the causing factors can generally be classified into geological and blasting factors.

　The geological conditions are given and uncontrollable factors which have a significant influence to overbreak phenomenon. Jang and Topal investigated the parameter contributions on uneven break (UB: overbreak and underbreak) phenomenon in underground stoping mines[2]. The study reveals that the sum of two geological

parameters (the adjusted Q-value and the in-situ stress value K) comprises 38.6 % of UB contribution among ten other factors including stope design and blasting factors. It is a common understanding that if the rock is not strong enough to sustain itself, the overbreak due to blasting is inevitable. In contrast, blasting parameters are manageable factors. Many controlled blasting methods have been introduced by trial and error in practice. Smooth blasting method is the typical method to overbreak control in underground tunnel blasting where the line of perimeter holes with a light charge fire at the end of the blasting round. Also, automated drilling systems and various trim blast customised explosives for decoupling charge maximise the effect of the smooth blasting principles.

　The quality of tunnel contour control is principally dependent on the design of perimeter spacing-to-burden (from here, spacing-to-burden donate only perimeter hole
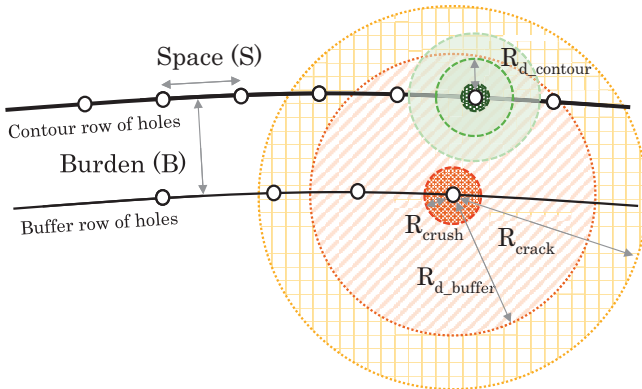
Figure 1   Diagrammatic view of blast damage zone (BDZ) from contour and buffer hole.

spacing-to-burden). Moreover, it should be noted that the primary function of perimeter holes is not breaking the rock mass but smoothing the contour[3]. Figure 1 demonstrates tunnel contour design and possible blast damage zones (BDZ) from the perimeter and buffer hole.

For a good contour control with the smooth blasting method, spacing-to-burden (S/B) ratio should be maintained less than or equal to 0.8. The controlled explosive pressure using the decoupling charge with shorter space of perimeter holes fosters to create tensile cracks between the holes. The borehole pressure of perimeter holes should be maintained less than the compressive strength of the rock to avoid compressive failures around the holes. If spacing is too long, it may not create tensile cracks across the perimeter holes. Moreover, the influence of geological fractures can be enhanced which disturbances to create a smooth wall. Conversely, short spacing will increase drilling cost. Consequently, the perimeter spacing-to-burden (S/B) ratio design is critical to maintaining a smooth contour.

The study aims to evaluate the perimeter spacing-to-burden ratio for a standard tunnel blasting design for 1 m advance used in a tunnel construction site in Japan, where the S/B ratio is 1.14 as the perimeter space and burden are 0.83 and 0.73 m respectively. The current perimeter S/B design was compared with blast damage models from Ash[4]. In succession, a nonlinear hydro-code, AUTODYN was used to simulate five models with different S/B design to compare fracture propagation results. Through the study, it also can be verified the BDZ estimation using numerical analysis comparing with the Ash's BDZ approaches.

Section 2 demonstrates eminent BDZ calculation models. Section 3 briefly reviews constitutive material models studied for rock behaviour under dynamic blast loading. Section 4 introduces numerical analysis and applied material models. Section 5 discussed the results of BDZ models comparing with current perimeter S/B design in practice and the numerical analysis results. Section 6 concludes the study representing essential findings.

2. Blasting damage zone models
Sjoberg et al. investigated the depth of blast-induced damage in road tunnels[5],[6]. The damage depth was measured in coring holes on the tunnel inverts with the damage criterion of two new fractures per meter of coring hole. The work has long been used for the judgement of BDZ in tunnel projects in Sweden and has been published as 'the Swedish table of damage zone depth' in 1995[7]. The table is valid for borehole diameter ranges of 45 to 51 mm and decoupling change, bulk emulsion, and water effects have not been regarded[8].

Holmberg and Persson introduced a BDZ model where rock damage is described by peak particle velocity (PPV) which is proportional to the resultant of the induced strain in an elastic medium[9]. In the model, PPV damage criterion of 700−1000 mm·s^{-1} was used to predict BDZ. Later on, Hustrulid introduced the buffer concept for tunnel perimeter control design which is similar to Holmberg's work[10]. In the buffer concept, the burden should be maintained less than the practical damage radius of the buffer hole (R_{d_buffer}). So, the BDZ caused by a buffer hole is not exceeded beyond the practical blast damage zone of the perimeter hole. Indeed, a proper burden by the practical blast damage zone radius of the buffer hole is the key to maintain overbreak in tunnel blasting.

Ash proposed BDZ models utilising field blasting operation data[4]. Ash's first BDZ model is called 'Modified Energy-based model' that defines a relationship between the bulk strength of explosive and the ratio of practical damage radius (r_0) per borehole radius (r_h). The energy-based BDZ model initially assumed the fully coupled charge, and it was updated later to calculate BDZ of decoupled charges. The advantage of the model is that the BDZ can easily estimate with the density of explosive and rock. Second Ash's BDZ model is 'Modified Pressure-based model' which includes the borehole pressure (P_h) in consideration.

Sher introduced a BDZ model for a cylindrical fully coupled charge based on quasi-static mechanics which requires different rock parameters[11],[12]. The advantage of Sher's BDZ model is that it can estimate BDZs in different rock compressive strengths and explosive pressure. However, it can become a disadvantage if rock parameters are not available. Besides, Sher's model produces relatively comparable results with Ash's modified Pressure-based model.

3. Rock material models for dynamic rock failures
Numerous studies have been conducted to develop adequate constitutive material models to understand rock failure behaviours under dynamic blast loading. The rock breakage mechanism due to dynamic blast loading cannot be fully explained either with the impulsive loading by stress waves or gas pressure drove fracture propagation. It is still controversial, but the shock waves can be considered as the primary source of creating rock fractures based on the fact that it travels much faster than the gas pressure. In fact, many studies considered the stress-induced rock fracturing where the damage models based on gas pressurisation are infrequently studied[13]−[17].

Tayler introduced a constitutive model (CTK model) that simulates stress wave-induced dynamic rock fracture behaviour of oil shale[18]. In the model, the stress-induced micro crack due to volumetric tensile loading affected by the strain rate leaves portions of rock volume unable to carry the load. In other words, the CTK model simplifies the inelastic behaviour under compression as an elastic-perfectly-plastic response. Yang argued that Taylor's model in which mean normal stress was adopted to characterise between brittle cracking and compressive crushing could not account for several brittle failure modes[19]. Later, Yang introduced a constitutive model that can reasonably model various failure modes by assuming the brittle failure under dynamic blast loading is governed by the extensional strain. Liu developed a constitutive model to predict rock damage due to dynamic blast loading based on a continuum and statistical fracture mechanics[20]. Liu's model assumed the rock is under an isotropic, continuous, and homogeneous condition with inherent microcracks. The damage was defined as the probability of fracture at a given crack density. Ma suggested a dynamic rock failure model based on thermodynamics theory incorporating with a piecewise linear DruckerPrager strength criterion and anisotropic continuum damage model[21].

RHT material model is introduced by Riedel, Hiermaier, and Thoma[22] which is a compressive-tensile damage model for concrete and rock-like materials. The RHT model used the P-α compaction model as the equation of state (EOS). The model describes the constitutive relation between pressure and volumetric strain, which characterises irreversible compaction behaviours at low pressure and the correct Hugoniot description at high pressure. More comprehensive details of the P-α compaction model can be found in Herrmann[23] and Collins's work[24]. The RHT model was developed on the basis of the Johnson-Holmquist (JH) model[25],[26]. Thus, it has similar descriptions of the strain rate effects and the damage variables with JH. The main difference is that the RHT model considers the stress deviator tensor (J_3) by constructing different tensile and compressive meridians[27]. More details of RHT model is described in Section 4.

The inherent characteristics of rock discontinuous, such as joint, bedding, cleavages, and schistosity have critical influences to the behaviour of rock damage and crack propagations due to the dynamic blast loading which cannot be captured in the isotropic damage model. Hao studied an anisotropic continuum damage model due to blast-induced stress[28]. The model developed based on the theory of continuum damage mechanics where cumulative rock damage was evaluated by the exponential function of the principal tensile strain. Zhang conducted a study to develop a constitutive model that can predict the dynamic anisotropic damage in brittle rock-like materials under the dynamic blast loading[29]. The model introduced a second rank symmetric damage tensor to take account the anisotropy of damage that is depending on an equivalent tensile strain.

4. Numerical simulation and material models

The standard blasting design for 1 m advance has been adopted from HAZAMA ANDO CORPORATION. The tunnel blasting carries on with the normal profiling method where the same explosive charge pattern is applied to stoping, buffer, and contour holes.

Five simulation models have been prepared to elucidate the effect of S/B ratio to overbreak phenomenon. Each model is composed of three perimeter and two buffer holes in different S/B ratios from 0.6 to 1.4. In the model, the perimeter hole space and the buffer hole burden are fixed to 830 mm and 730 mm respectively. Thus, the S/B ratio of the simulation model is only a function of the perimeter burden. The perimeter burden and S/B ratio of five models are tabulated in Table 1. Also, The Figure 2, (a), (b), and (c) show a graphical view of the model No. 1, the upper section dimension of the standard tunnel design, and the S/B ratio of five simulation models compared with the current model respectively.

In AUTODYN 2D, rock mass was modelled with Lagrangian elements including ϕ 45 mm of three perimeter and two buffer holes. The five holes were initially filled with air using Euler elements, then ϕ 30 mm emulsion explosive material model is filled in the centre of air elements. All holes were charged with the coupling ratio in diameter ($C_d = (d_{explosive}/d_{borehole})$) of 0.67 as customised explosives for decoupling charge are not applied to perimeter holes in practice. All models have been designed with the same scale using around 220,000 to 250,000 elements.

4.1 Rock and explosive material models

The numerical simulation of blast loading on rock-like materials requires Equation of State (EOS) and appropriate material constitutive model that can reflect the dynamic nonlinear behaviour of materials at high strain rate. In the study, RHT material model[22] is applied using AUTODYN code. Figure 3 shows the limited surfaces in the deviatoric stress space[30].

In the RHT model, the material is elastic until the stress reaches the elastic limit surface (Y_{el}). Beyond the elastic stress limit, the material starts to behave plastically as plastic strains evolve with a linear hardening properties. When the stress reaches the failure surface (Y_{fail}), the plastic strain drives the damage of the material until the accumulated plastic strain ($\Delta\varepsilon^p$) equals to the failure strain (ε^f), where the residual strength surface (Y_{res}) in Figure 3. Thus, the damage level of the RHT model is defined as $D = (\Delta\varepsilon^p/\varepsilon^f)$ which is 0 and 1 at the failure and residual strength surface respectively.

In the study, Barre granite (BG) is selected to evaluate the standard blasting design. The RHT material parameters of BG were adopted from Banadaki and Xie's

Table 1   Burden and S/B ratio of simulation models.

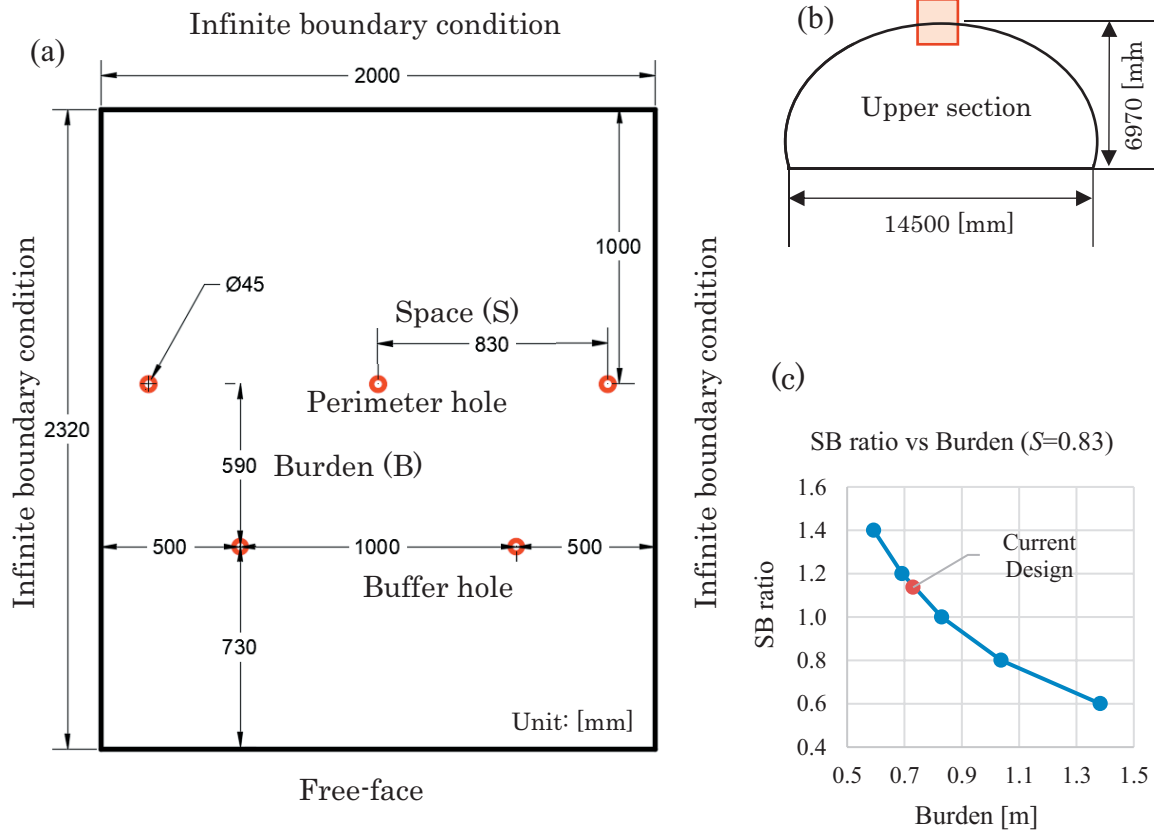| Model No.	1	2	3	4	5
B	0.59	0.69	0.83	1.04	1.38
S/B ratio	1.4	1.2	1	0.8	0.6

Figure 2   Details of the simulation model (a) a graphical view of the model No. 1, (b) dimension of the upper section of the standard tunnel design, (c) *S/B* ratio of simulation models and the current blasting design.
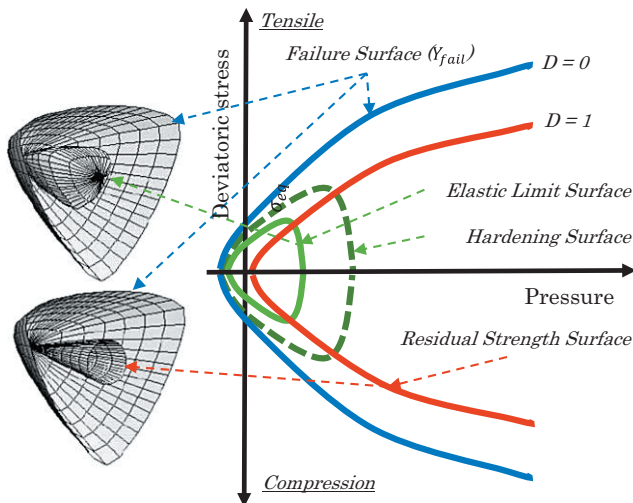

Figure 3   Three limited surfaces in deviatoric stress space after Riedel (2009).

studies in which these parameters were calibrated with a series of laboratory blasting experiments[31),32)]. RHT material parameters for the Barre granite in Lagrange elements for AUTODYN simulation are tabulated in Table 2.

An emulsion explosive, Titan-6000-E6[33)], was applied to the numerical model in AUTODYN with JWL model as it has similar properties with ULTEX®[34)] which is commonly used in Japan. The equation of state (EOS) of JWL is expressed in Equation 1, and the explosive material parameters for JWL model are tabulated in Table 3.

$$P = A\left(1 - \frac{\omega}{R_1 V}\right)e^{-R_1 V} + B\left(1 - \frac{\omega}{R_2 V}\right)e^{-R_2 V} + \frac{\omega E}{V} \quad (1)$$

Where P is the detonation pressure, V and E are the specific volume and the internal energy of the detonation products respectively, and A, B, R_1, R_2, and ω are constants.

5. Blast damage zone evaluation and discussions

The practical damage zone of the standard tunnel design has been evaluated applying Ash's modified energy-base and pressure-base approaches. In addition, the five models with different *S/B* ratio have been simulated using AUTODYN, ANSYS to compare with Ash's BDZ approaches. The Holmberg-Persson BDZ model has not been considered as the model cannot be appropriately calibrated for the study case.

5.1 Ash's BDZ approach

Modified Energy and pressure based models have been applied to estimate BDZ of the original tunnel perimeter design. The BDZ can be estimated using modified Ash's energy-based model from:

$$\frac{r_0}{r_h} = 25 \cdot \sqrt{\frac{\rho_e \cdot s_{ANFO}}{\rho_{ANFO}}\left(\frac{A_e}{A_h}\right)} \cdot \sqrt{\frac{2.65}{\rho_{rock}}} \quad (2)$$

Where, ρ_e, ρ_{ANFO}, and ρ_{rock} are the density of the explosive, ANFO, and rock in g·cm^{-3}. A_e and A_h are the cross sectional area of the explosive and the borehole respectively. In the equation, ρ_{ANFO} is assigned to 0.85 and

Table 2   RHT model parameters of Barre granite in Lagrangian elements for AUTODYN.

P-α EOS parameters		Intact failure surface constant, B_{fail}	2.44
Mass density	2.66×10^3 [kg·m^{-3}]	Intact failure surface exponent, N_{fail}	7.60×10^{-1}
Crush pressure	1.25×10^2 [GPa]	Tens./Comp. Meridian ratio, Q	6.80×10^{-1}
Compaction pressure	6.00 [GPa]	Brittle to ductile transition	5.00×10^{-2}
Bulk modulus, A_1	2.57×10^1 [GPa]	Comp. strain rate Exp., α_{sr}	2.60×10^{-2}
Bulk modulus, A_2	3.78×10^1 [GPa]	Tensile strain rate Exp., δ_{sr}	7.00×10^{-3}
Bulk modulus, A_3	2.13×10^1 [GPa]	Elastic strength / f_c	5.30×10^{-1}
Pore crush, B_0	1.22	Elastic strength / f_t	7.00×10^{-1}
Pore crush, B_1	1.22	G (elas.)/(elas.-plas.)	2.00
Bulk modulus, T_1	2.57×10^1 [GPa]	Fracture strength constant, B_{fric}	2.50×10^{-1}
Bulk modulus, T_2	0.00	Fracture strength exponent, N_{fric}	6.20×10^{-1}
Specific heat*	7.90×10^2 [J·kgK^{-1}]	Failure Parameters	
Thermal conductivity**	3.07 [W·mK^{-1}]	Damage constant, D_1	4.00×10^{-2}
Strength parameters		Damage constant, D_2	1.00
Elastic Shear modulus, G	2.19×10^1 [GPa]	Minimum strain to failure	1.50×10^{-2}
compressive strength, f_c	1.68×10^2 [MPa]	Residual shear modulus fraction	1.00
Relative tensile strength, f_t/f_c	4.00×10^{-2}	Erosion plastic strain	1.50
Relative shear strength, f_s/f_c	2.10×10^{-1}	Tensile Failure	Hydro (P$_{min}$)

*Specific heat of granite referred from Engineering_ToolBox[36], **Thermal conductivity of granite referred from Sharma[37]

Table 3   JWL model parameters of Titan-6000-E6.

ρ_0 [kg·m^{-3}]	VOD [m·s^{-1}]	P_{CJ} [GPa]	A [GPa]	B [GPa]	R_1	R_2	ω	E_0 [GPa]
1130	6031	9.558	365.290	2.703	4.999	0.892	0.23	3.036

VOD: Velocity of detonation

2.65 denotes the average density of rock delivered from Ash's work when a light explosive is used in the average rock condition. The advantage of the model is that the BDZ can easily estimate with the density of explosive and rock. Second Ash's BDZ model is 'Modified Pressure-based model' which includes the borehole pressure (P_h) in consideration. The equation is similar with the Ash's pressure-based BDZ model as it is shown in Equation (3).

$$\frac{r_0}{r_h} = 25 \cdot \sqrt{\frac{P_h}{P_{ANFO}}} \cdot \sqrt{\frac{2.65}{\rho_{rock}}} \tag{3}$$

Where P_{ANFO} signifies the borehole pressure of 1300 MPa that is derived from the full coupled charge of ANFO with density and VOD are 0.85 and VOD 3500 m·s^{-1}, respectively.

The density and velocity of detonation (VOD) of ULTEX are 1.19 g·m^{-3} and 5900 m·sec^{-1}, respectively. The absolute weight strength of ULTEX is 771.95 cal·g^{-1}, and the S$_{ANFO}$ is calculated at 0.84. Decoupling ratio (A_e/A_h) is 0.44 as the ϕ 30 mm of explosive is charged into the ϕ 45 mm of borehole. ρ_{rock} is assumed as 2.66 as same as the Barre granite. Under the condition, BDZ (r_0) based on Ash's modified Energy and pressure based models are calculated as 0.81 m and 0.95 m.

5.2 BDZ estimation through AUTODYN

Five models with different *S/B* ratio demonstrated in Table 1 and Figure 2 have been simulated using AUTODYN, ANSYS. The initiation delay time between the buffer and the perimeter row of holes is 25 ms in the standard tunnel design. However, in the numerical modelling, it is difficult to run the model in such a long time as elements will be undergoing substantial distortions, which can stop the simulation[35]. As the aim of the study is to investigate *S/B* ratio effects to the overbreak phenomenon, the time delay between the perimeter and buffer row of holes is set to 1 ms. It also need to be mentioned that the length of the blast hole and the lookout angel on perimeter holes have not been considered as the study used 2D finite element model for investigating the *S/B* ratio effects to perimeter rock break. AUTODYN simulation results of the five models in 0.5, 1.0, 1.5, and 2.0 ms are demonstrated in Table 4.

The blast loading from two buffer holes causes severe compressive damages around the buffer holes, and several radial cracks are extended further to the rock mass. Severe tensile failures are observed near the free face due to reflected tensile waves. In addition, the shock waves from the buffer hole blast create vertical tensile cracks on the perimeter holes which extended further into the rock mass after initiating perimeter holes. The vertical tensile cracks observed on the all three perimeter holes in model 1 and 2 as shown in 0.5 ms column in Table 4 with red-dot circles. It appears at only the center perimeter hole in model 3 and 4 due to interactions of blast loads from the two buffer holes. In this study, the practical blast damage zone (BDZ) of the numerical simulation using AUTODYN is defined as 'the minimum length of the multiple cracks from the center of the blast hole excepting extended cracks influenced by the perimeter holes'. The BDZs are examined with the simulation results at 1.0 ms of five models when the blast loading from the buffer holes are

Table 4   AUTODYN simulation results of five models at 0.5, 1.0, 1.5, and 2.0 ms.

| Damage Level | 0.1 | 0.2 | 0.3 | 0.4 | 0.5 | 0.6 | 0.7 | 0.8 | 0.9 | 1.0 |
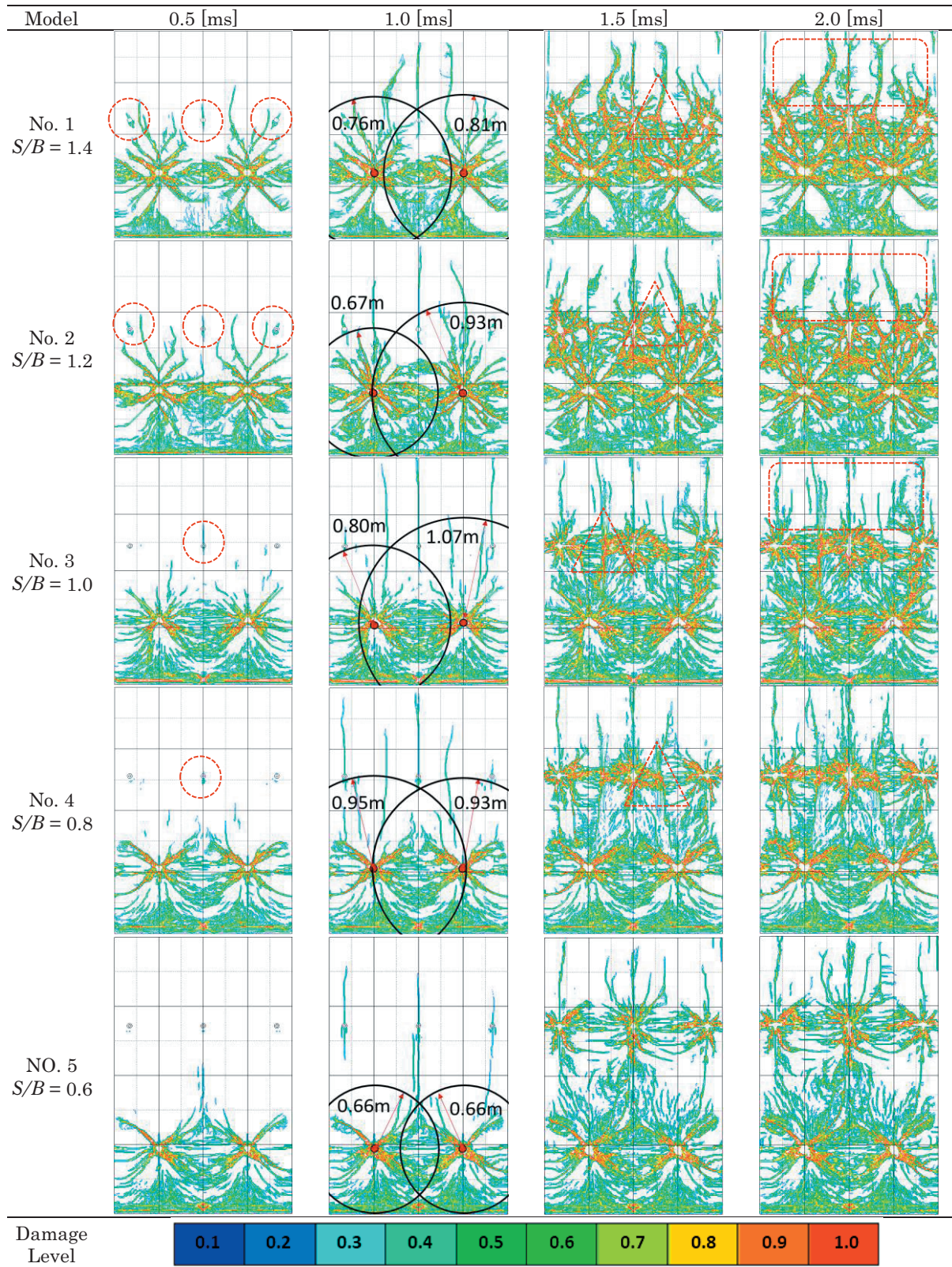
finalized. The examined BDZ of numerical simulation are noted in 1.0 ms column in Table 4, and the average BDZ by the numerical analysis is 0.82 m.

The vertical tensile cracks extended into the rock mass beyond the tunnel contour hinder the growth of tensile cracks along with the perimeter line as shown as red-dot triangles in 1.5 ms column in Table 4. It also observed that the formulated vertical tensile cracks cross over the perimeter line exacerbate damages. In addition, high-level damages ($D \leqq 1$) more likely appear when S/B ratio is over 1.0 as shown as red-dot boxes in 2.0 ms column in Table 4.

5.3 BDZ comparisons

The BDZs estimated through Ash's modified energy and pressure-based approaches which are compared with the numerical simulation results of five models at 2.0 ms as shown in Table 5.

Table 5   Comparisons BDZ results from the numerical simulation using AUTODYN, Ash's modified energy-based, and Ash's modified pressure-based approaches in five models at 2.0 ms.
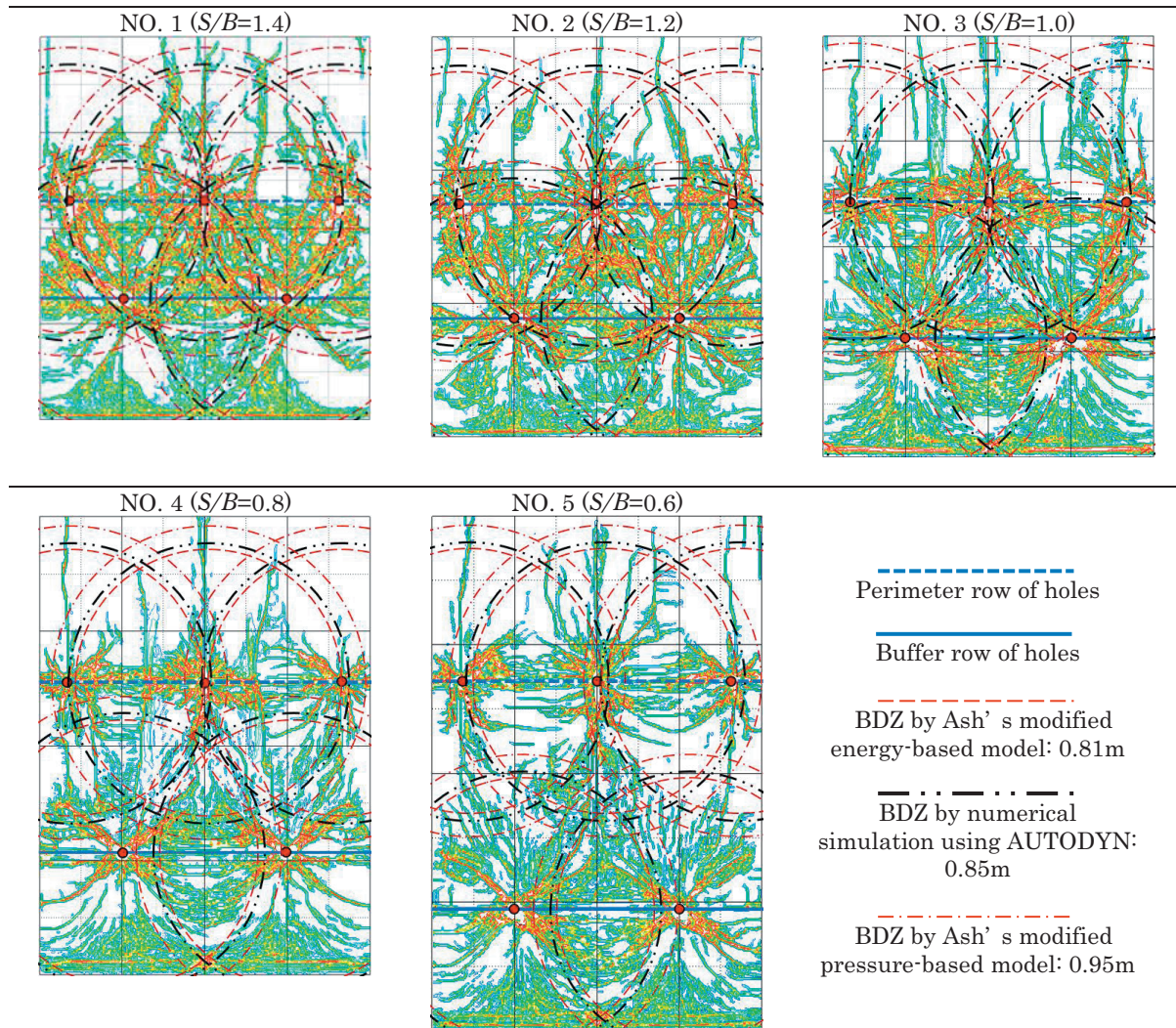
The BDZ estimation approaches used in this study produced similar results. BDZ of the Ash's modified-energy, modified-pressure, and the average of the Autodyn simulation are 0.81 m, 0.95 m and 0.82 m, respectively. As shown in Table 5, BDZs estimated from the four approaches are crossed over the perimeter row of holes in model 1 and 2. Contrastively, estimated BDZs are shorter than perimeter burden of model 4 and 5. Given that the buffer concept, the most appropriate tunnel perimeter S/B design for the standard tunnel design for 1 m advance of the tunnel construction site is model No. 3 when $S/B = 1.0$ as the perimeter burden and the average BDZs are equal to 0.83 m.

6. Conclusions

The study aims to evaluate the perimeter S/B ratio of the standard blasting design used in a tunnel construction site in Japan, where the perimeter S/B ratio is 1.14 as the perimeter space and burden are 0.83 m and 0.73 m, respectively. The buffer concept from Hustrulid and Johnson's study was considered in the study to verify an appropriate S/B ratio of the tunnel blasting design used in the construction site in Japan. First, blast damage zone (BDZ) of a single blast hole is estimated using Ash's

modified energy and pressure-based approaches which calculated as 0.81 and 0.95 m, respectively.

In succession, five numerical models with different S/B designs are prepared to simulate rock mass damages due to blast loads from two buffer and three perimeter holes using a nonlinear hydro-code, AUTODYN, ANSYS with the RHT material model, and JWL EOS model. The delay time between the buffer and the perimeter row of holes was set to 1 ms. The impulsive blast loading from the two buffer holes created vertical tensile cracks over the perimeter line. The tensile cracks appeared in perimeter holes extended further into the rock mass after initiating perimeter holes. The vertical tensile cracks between the perimeter holes hinder the growth of tensile cracks along with the perimeter line. In the study, the practical blast damage zone of the numerical analysis is defined as 'the minimum length of the multiple cracks from the center of the blast hole excepting extended cracks influenced by the perimeter holes', and the average practical BDZ of the numerical analyses was computed as 0.83 m.

Results show that the BDZ estimation using the numerical analysis is reasonably corresponding with the Ash's BDZ approaches. Through the study, the most appropriate perimeter S/B ratio of the tunnel blasting

design of the site is 1.0 which gives appropriate fractures at the area between the buffer and the perimeter row of holes with suspending excessive overbreak the tunnel contour. The presented process of the BDZ evaluation can be applied in tunnel blasting designs in practice to minimize possible overbreak.

Acknowledgements

References

1) H. Jang and E. Topal, Tunn. Undergr. Sp. Tech., 38, 0, 161–169 (2013).
2) H. Jang, E. Topal, and Y. Kawamura, Int. J. Min. Sci. Technol., 26, 1095–1100 (2016).
3) S. Iverson and W. Hustrulid, 45th US Rock Mechanics/ Geomechanics Symposium, American Rock Mechanics Association, (2011).
4) R. L. Ash, Pit and quarry, 56, 11 (1963).
5) C. Sjoberg, B. Larsson, M. Lindstrom, and K. Palmqvist, A blasting method for controlled crack extension and safety underground, ASF project, 77/224 (1977).
6) C. Sjoberg, Proceedings of annual discussion meeting BK–79. Swedish rock construction committee, Stockholm, 53–98 (1979).
7) SNRA, Cautious blasting, careful blasting and scaling, rock engineering directions for the construction of Ringen and Yttre Tvärleden. In: Administration SNR, ed. Project directions ANV 00031:1; 1st rev. Stockholm (1995).
8) F. Ouchterlony, M. Olsson, and I. Bergqvist, Fragblast, 6, 235–261 (2002).
9) R. Holmberg and P.–A. Persson, Proceedings, Tunneling, 79 (1979).
10) W. A. Hustrulid, Underground mining methods handbook (1982).
11) E. Sher, J. Appl. Mech. Tech. Ph., 38, 484–492 (1997).
12) E. Sher, N. Aleksandrova, M. Ayzenberg-Stepanenko, and A. Chernikov, J. Min. Sci., 43, 585–591 (2007).
13) J. Dally, W. Fourney, and D. Holloway, Int. J. Rock Mech. Min., 5–12, 12. Elsevier (1975).
14) S. McHugh, Int. J. Fract., 21, 163–176 (1983).
15) A. S. Paine and C. P. Please, Int. J. Rock Mech. Min., 31, 699–706 (1994).
16) Y. J. Ning, J. Yang, G. W. Ma, and P. W. Chen, Rock Mech. Rock Eng., 44, 483–490 (2011).
17) F. García Bastante, L. Alejano, and J. González-Cao, Int. J. Rock Mech. Min., 56, 44–53 (2012).
18) L. M. Taylor, E. P. Chen, and J. S. Kuszmaul, Comput. Method Appl. M., 55, 301–320 (1986).
19) R. Yang, W. F. Bawden, and P. D. Katsabanis, Int. J. Rock Mech. Min., 33, 245–254 (1996).
20) L. Liu and P. D. Katsabanis, Int. J. Rock Mech. Min., 34, 217–231 (1997).
21) G. W. Ma, H. Hao, and Y. X. Zhou, Comput. Geotech., 22, 283–303 (1998).
22) W. Riedel, "â Beton Unter Dynamischen Lasten: Meso-Und Makromechanische Modelle Und Ihre Parameter, Fraunhoferâ Ernst-Mach-Institut, Freiburg/Br" ISBN 3–8167–6340–5, (2004).
23) W. Herrmann, J. Appl. Phys., 40, 2490–2499 (1969).
24) G. Collins, H. Melosh, and K. Wünnemann, Int. J. Impact. Eng., 38, 434–439 (2011).
25) G. R. Johnson and T. J. Holmquist, AIP Conference Proceedings, 981–984, 309. American Institute of Physics, (1994).
26) T. J. Holmquist and G. R. Johnson, J. Appl. Mech., 78, 051003 (2011).
27) X. Zhou, V. Kuznetsov, H. Hao, and J. Waschl, Int. J. Impact. Eng., 35, 1186–1200 (2008).
28) H. Hao, C. Wu, and Y. Zhou, Rock Mech. Rock Eng., 35, 79–94 (2002).
29) Y.-Q. Zhang, H. Hao, and Y. Lu, Int. J. Eng. Sci., 41, 917–929 (2003).
30) W. Riedel, 10 years RHT: a review of concrete modelling and hydrocode applications. "Predictive modeling of dynamic processes": Springer: 143–165 (2009).
31) M. D. Banadaki and B. Mohanty, Int. J. Impact. Eng., 40–41, 16–25 (2012).
32) L. Xie, W. Lu, Q. Zhang, Q. Jiang, M. Chen, and J. Zhao, Tunn. Undergr. Sp. Tech., 66, 19–33 (2017).
33) J. A. Sanchidrián, R. Castedo, L. M. López, P. Segarra, and A. P. Santos, Cent. Eur. J. Energ. Mat., 12, 177–194 (2015).
34) J. Kayaku, "ULTEX", http://www.kayakujapan.co.jp, (accessed: 10-Sep-2019). (online).
35) C. Yi, J. Sjöberg, and D. Johansson, Tunn. Undergr. Sp. Tech., 68, 167–173 (2017).
36) Engineering_ToolBox, "Specific Heat of Solids", https://www.engineeringtoolbox.com/specific-heat-solids-d_154.html, (accessed: 10-Sep-2019). (online).
37) P. Sharma, "Environmental and engineering geophysics Cambridge University Press Cambridge" United Kingdom (1997).